Seasonal ice loss in the Beaufort Sea: Toward synchrony and prediction

Michael Steele[1], Suzanne Dickinson[1], Jinlun Zhang[1], and Ron W. Lindsay[1]

[1]Polar Science Center, Applied Physics Laboratory, University of Washington, Seattle, Washington, USA

Abstract The seasonal evolution of sea ice loss in the Beaufort Sea during 1979–2012 is examined, focusing on differences between eastern and western sectors. Two stages in ice loss are identified: the Day of Opening (DOO) is defined as the spring decrease in ice concentration from its winter maximum below a value of 0.8 areal concentration; the Day of Retreat (DOR) is the summer decrease below 0.15 concentration. We consider three aspects of the subject, i.e., (i) the long-term mean, (ii) long-term linear trends, and (iii) interannual variability. We find that in the mean, DOO occurs earliest in the eastern Beaufort Sea (EBS) owing to easterly winds which act to thin the ice there, relative to the western Beaufort Sea (WBS) where ice has been generally thicker. There is no significant long-term trend in EBS DOO, although WBS DOO is in fact trending toward earlier dates. This means that spatial differences in DOO across the Beaufort Sea have been shrinking over the past 33 years, i.e., these dates are becoming more synchronous, a situation which may impact human and marine mammal activity in the area. Retreat dates are also becoming more synchronous, although with no statistical significance over the studied time period. Finally, we find that in any given year, an increase in monthly mean easterly winds of ~1 m/s during spring is associated with earlier summer DOR of 6–15 days, offering predictive capability with 2–4 months lead time.

1. Introduction

Why does sea ice concentration decline each spring and summer in the Arctic Ocean? If the answer was solely thermodynamic melt driven largely by radiation fluxes, then (in the absence of persistent cloud and surface albedo anomalies) the pattern of ice loss should be zonally symmetric, with earlier reductions in the south and later reductions to the north [*Lindsay*, 1998]. In fact, the actual spatial pattern of ice reduction is more complex. Figure 1 shows climatological mean ice concentration decline in the Beaufort Sea during spring and early summer. The earliest ice loss occurs in the eastern Beaufort Sea (EBS), relative to later concentration declines in the western Beaufort Sea (WBS).

The EBS is defined here as shown in Figure 1, i.e., by longitudes 120°W–135°W and from the North American mainland coast north to 74°N. The eastern part of this domain includes most of Amundsen Gulf, where landfast ice dominates [*Galley et al.*, 2012; *Peterson et al.*, 2008]. We define the WBS with the same north-south boundaries as for the EBS, and by longitudes 135°W west to near Point Barrow at 155°W. The border between the two regions is set at 135°W, the southern-most point along the mainland coast and the western edge of the Mackenzie River delta. Figure 1 indicates that the WBS experiences a relatively late sea ice opening in a typical summer.

The initial stage of ice loss in the EBS is often identified as the Cape Bathurst Polynya, which first appears in ice concentration maps in May on the west sides of Banks Island, Amundsen Gulf, and Cape Bathurst (Figure 1) [*Barber and Hanesiak*, 2004]. This area provides a site for phytoplankton blooms and is thus of interest to arctic ecologists [*Arrigo and van Dijken*, 2004; *Carmack et al.*, 2004; *Simpson et al.*, 2013]. The polynya forms as spring easterly surface winds drive sea ice westward, away from Banks Island, the fast ice in Amundsen Gulf, and the west side of Cape Bathurst [*Markham*, 1975]. On a broader scale, *Lukovich and Barber* [2005] note the strong correlation between wind forcing and sea ice concentrations in this area. With regard to thermodynamic factors, *Tivy et al.* [2011] show a weak correlation between winter air temperatures (which influence ice thickness at the start of the melt season) and summer ice concentration in the eastern part of the EBS, while on the other hand *Lukovich and Barber* [2005] find little influence from air temperature forcing. *Williams and Carmack* [2008] show that upwelling of warm ocean water slows winter ice growth, but
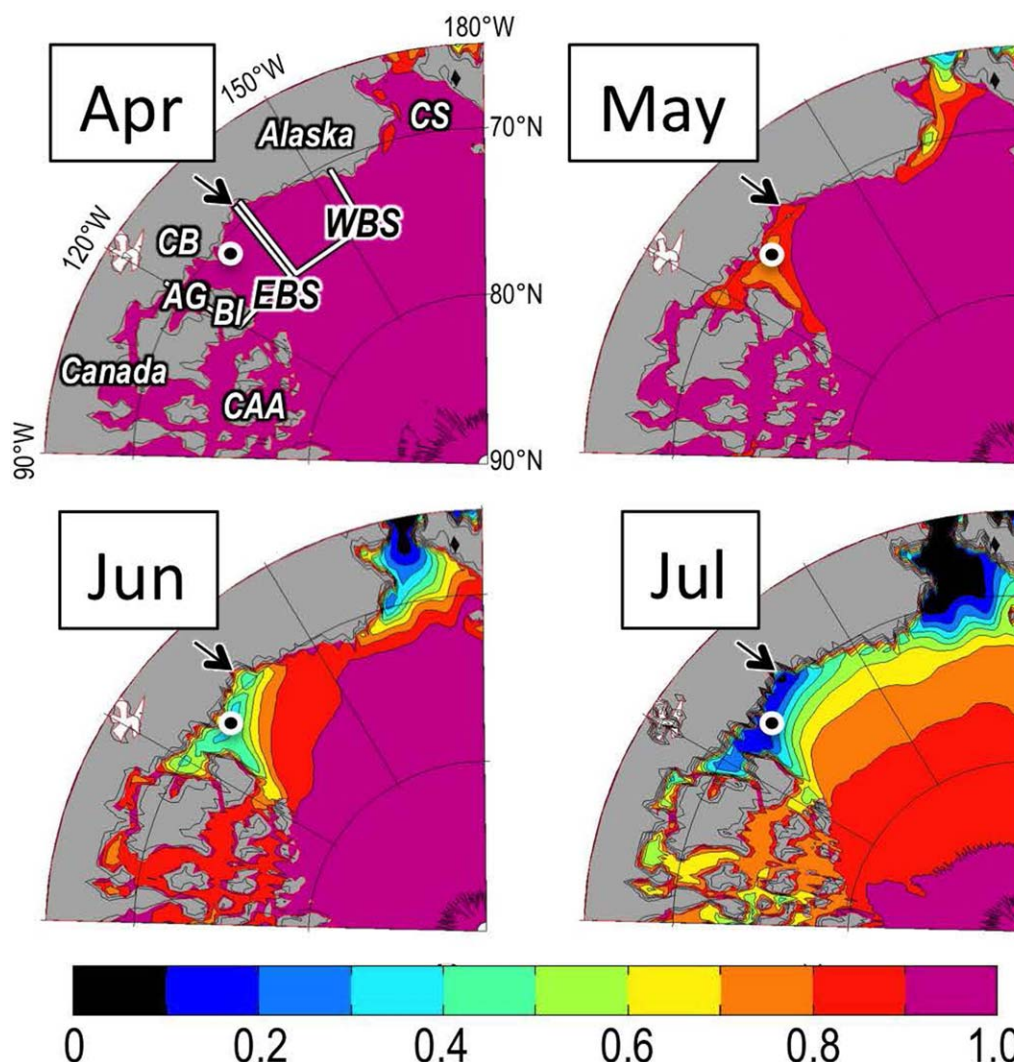
Figure 1. Monthly mean ice concentration for April, May, June, and July, averaged over the years 1979–2012, from National Snow and Ice Data Center (NSIDC) passive microwave data (http://nsidc.org/data/nsidc-0051.html, downloaded 30 July 2013). The eastern Beaufort Sea (EBS) is bounded by the coast north to 74°N and longitudes 120°W–135°W; the western Beaufort Sea (WBS) is similar but bounded by longitudes 135°W–155°W. The boundary between the two regions lies at the southern-most point along the coastline, which is also the western edge of the Mackenzie River delta (black arrow). Also noted are the Chukchi Sea (CS), Canadian Arctic Archipelago (CAA), Banks Island (BI), Amundsen Gulf (AG), Cape Bathurst (CB), and the center of low ice concentration in June at 71°N, 130°W (dot).

only as a transient phenomenon in localized areas. *Nghiem et al.* [2014] show that Mackenzie River discharge can melt ice, although this only starts in June in the western part of the EBS region.

Over the past 40 years, arctic summer sea ice concentration has been generally decreasing [*Comiso and Hall*, 2014], but long-term trends in this decrease are not zonally symmetric around the Arctic Ocean. In the Beaufort Sea, summer ice concentration is declining in the west, with weaker trends in the east [*Tivy et al.*, 2011]. A similar result holds for the date of ice retreat, i.e., ice is retreating earlier in the WBS while there is no significant trend in the EBS [*Frey et al.*, 2014; *Stammerjohn et al.*, 2012].

In the present study, we explore in further detail some aspects of seasonal sea ice loss in the Beaufort Sea. Our focus is on "early season" i.e., spring and early summer, as opposed to mid/late summer and the sea ice minimum, which has been the focus of many previous studies [e.g., *Drobot and Maslanik*, 2003; *Hutchings and Rigor*, 2012]. We seek to answer the following questions: why is mean seasonal ice loss asynchronous across the Beaufort Sea? What are the implications of spatial differences in long-term ice loss trends on the timing of sea ice loss across the Beaufort Sea? Can yearly anomalies in sea ice loss be linked to anomalies in forcing earlier in that year? Section 2 presents our data and methods, including an introduction of two

stages of seasonal ice loss: "opening" and "retreat." In section 3, we revisit the mechanisms responsible for mean seasonal ice loss, partitioning these into dynamic versus thermodynamic processes. In section 4, we consider how east-west differences in ice loss trends impact east-west differences in the date of ice loss. In section 5, we explore the potential for predicting seasonal ice loss as a function of local wind forcing. Finally, section 6 provides a summary and discussion.

2. Methods

In this paper, we analyze satellite data, atmospheric data from weather stations and from reanalysis products, and numerical model output, all focused on sea ice properties and forcing in the Beaufort Sea. Ice concentration data were obtained from the National Snow and Ice Data Center (NSIDC) in Boulder, Colorado. This is a merged product using SMMR, SSM/I, and SSMIS passive microwave sensors processed with the NASA Team algorithm, provided at 25 km spatial resolution and as daily means after mid-1987, and 2 day means before then [*Cavalieri et al.*, 1996]. Concentration accuracy is provided by NSIDC (quoting [*Cavalieri et al.*, 1992]) as 5% in winter, 15% in summer, although this might be an underestimation in some areas of the Beaufort Sea [*Agnew and Howell*, 2003; *Tivy et al.*, 2011].

We also analyze 10 m surface winds, sea level pressure, and net shortwave surface fluxes from the NCEP/NCAR atmospheric reanalysis [*Kalnay et al.*, 1996]. We compared these fields with those from other reanalyses such as NASA's Modern-Era Retrospective Analysis for Research and Applications (MERRA), NCEP's North American Regional Reanalysis (NARR), DOE-NCEP's Reanalysis 2 (NCEP2), and ECMWF's operational product. While some differences are evident, the qualitative characteristics with respect to our analysis are similar for all. We use the NCEP/NCAR data for consistency with numerical model output forced in part by these fields (see next paragraph). This reanalysis has been used in a variety of studies on the role of wind forcing on sea ice concentration in the Beaufort Sea [*Barber and Hanesiak*, 2004; *Drobot and Maslanik*, 2003; *Lukovich and Barber*, 2005]. We also considered 10 m surface wind data collected near the EBS over the years 1979–2012 at meteorological stations in the communities of Tuktoyaktuk and Sachs Harbour, and over the years 1989–2012 in the community of Ulukhaktok (formerly, Holman). Hourly data (often with missing observations for part of the day) were first averaged into daily means, then into monthly means from which annual means and interannual trends were calculated.

Sea ice thickness and motion are provided here by the Parallel Ice-Ocean Modeling and Assimilation System (PIOMAS) [*Zhang and Rothrock*, 2003], a numerical sea ice—ocean model forced by the NCEP/NCAR atmospheric reanalysis fields. Specifically, we used the IC-SST run discussed in depth in *Schweiger et al.* [2011], wherein observed satellite sea ice concentration (IC) and sea surface temperature (SST) data are assimilated to provide an optimal state estimate of the upper ocean and sea ice fields. Ice thickness and motion have been carefully validated [*Schweiger et al.*, 2011; *Zhang et al.*, 2012], relative to in situ observations from buoys, moorings, surface and subsurface ships, and satellite data, to the extent that this run is taken as a "state estimate" by a number of investigators [*Chevallier et al.*, 2013; *Laxon et al.*, 2013; *Overland and Wang*, 2013; *Snape and Forster*, 2014]. Estimated model thickness bias (relative to ICESAT satellite ice thickness) is <0.1 m, while model ice motion bias (relative to buoy observations) is <1 cm/s. Time series correlation (r) with observations for both model parameters is >0.70. The bias in ice thickness trends compared to the sparse arctic-wide observational data set is $\sim$1–2 cm/yr, although this is possibly an upper limit given the model's particularly small thickness bias in the Beaufort Sea [*Schweiger et al.*, 2011]. As with most such models, PIOMAS does not explicitly follow ice age (e.g., first-year versus multiyear ice).

A time series of ice concentration during spring and summer in the Beaufort Sea can be generally described by three phases. Figure 2 shows four examples from a location in the EBS. The first phase reflects the end of the growth season, when ice concentration varies between 0.8 and 1.0 with no decreasing trend. The second phase describes the time of ice loss, when concentration drops to its seasonal minimum. This drop is rarely monotonic, and frequently shows temporary increases that are likely related to wind-forced advection of the mobile ice pack. The third and final phase is the open water or ice minimum state, when concentration drops to values generally below 0.15, the threshold frequently taken as the "ice edge" in the literature [e.g., *Frey et al.*, 2014]. Weekly mean time series of ice concentration for the nearby Amundsen Gulf (where fast ice dominates in winter) show similar, although more smoothed behavior [*Galley et al.*, 2008].

In recognition of this three-phase behavior, we here define two break points of sea ice loss. The first we refer to as the Date of Opening (DOO), which is the final date of the year when the unsmoothed ice
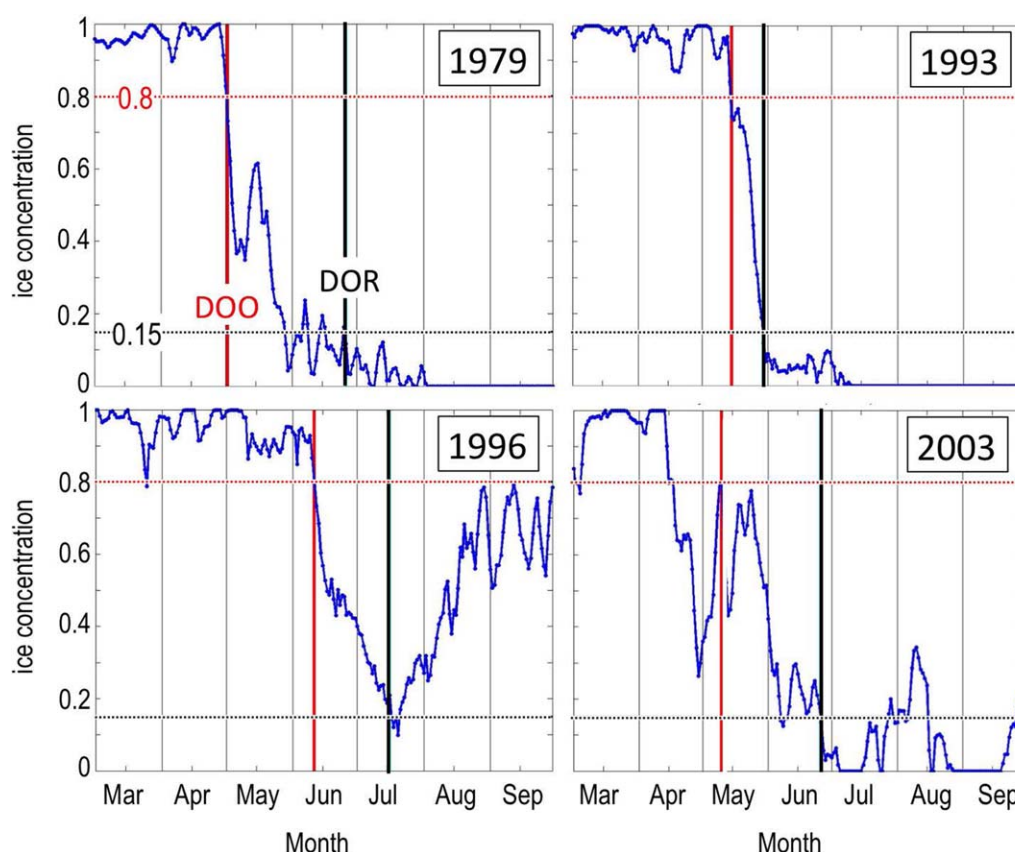
Figure 2. Time series of ice concentration (blue curve) at 71°N, 130°W during 4 years, using the same data as in Figure 1 except these are daily means (every other day for years before 1987). Also shown is the DOO (i.e., final date when concentration < 0.8, red lines) and DOR (final date when concentration < 0.15, black lines) for each year. The year 1979 shows a relatively long interval between DOO and DOR, with a temporary concentration increase in May. The year 1993 shows a very rapid and nearly monotonic ice loss. Ice loss in the year 1996 is also nearly monotonic, but never reaches zero concentration. The year 2003 provides a particularly "noisy" example when the definitions of DOO and DOR are not particularly valuable in describing ice loss.

concentration time series at a given location drops below a value of 0.8. This is a measure of the start of phase two, i.e., the start of the seasonal ice loss phase. Figure 3 shows DOO over the period 1979–2012 along latitude 71°N in the Beaufort Sea. There is a DOO for every longitude and every year in Figure 3, i.e., the ice concentration always drops below 0.80. In the mean, DOO happens at the end of May between longitudes 124°W and 132°W, while it is about 1 month later west of 140°W. Interannual variability in these dates is generally a bit lower in the EBS (±18–22 days) versus in the WBS (±20–26 days). Figure 3c shows a trend toward earlier opening everywhere in the Beaufort Sea, a result consistent with the general decline in arctic sea ice concentrations [e.g., *Cavalieri and Parkinson*, 2012]. However, these negative trends are weakest and least significant in the EBS, a result that will be discussed in further detail in section 4.

The second break point in seasonal sea ice loss will be defined here as the Date of Retreat (DOR), which is the final date when ice concentration drops below 0.15. This happens on average about 5 weeks later than DOO in the Beaufort Sea. It fails to happen along 71°N in the Beaufort Sea only about 4% of the time, and never after the year 1996. Interannual variance in DOR is about 50% greater than for DOO, while trends are of about the same magnitude for DOR and DOO. Over the years 1979–2012, the dates of ice opening and of ice retreat in any given year in the Beaufort Sea are highly correlated.

3. Mean Seasonality of Ice Opening

As described in section 1, previous work has highlighted the important role that wind forcing plays in the mean pattern of seasonal sea ice loss in the Beaufort Sea, although some role for thermodynamic factors has also been noted. Here we reexamine this issue, using both observations and model output in order to
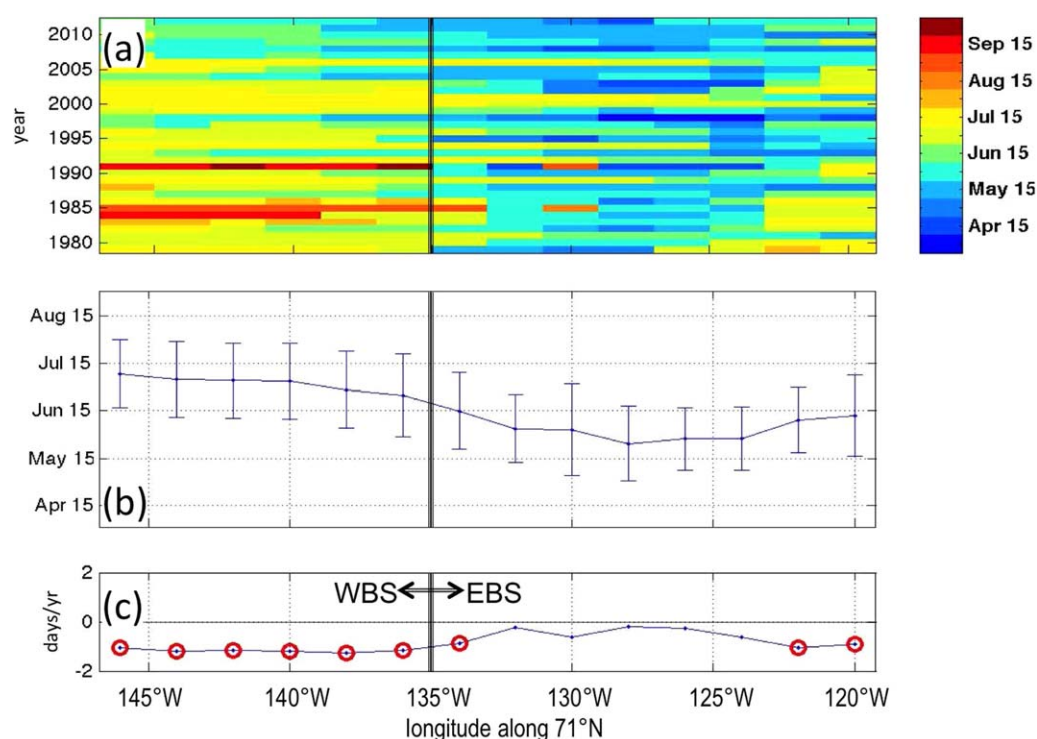
Figure 3. The variation along latitude 71°N of the Date of Opening, or DOO, defined as the final date of the year when ice concentration drops below 0.8, using the same data as Figure 1. Longitude 135°W marks the boundary between the western Beaufort Sea (WBS) and eastern Beaufort Sea (EBS). (a) Interannual variability during 1979–2012. (b) The long-term mean (line) and ±1 standard deviation of inter-annual variability (vertical bars). (c) The linear trend in days/yr; longitudes with at least 95% significance (F test) noted with red circles.

consider the key parameters of interest. In our study, autumn will be defined as October-November-December (OND), winter as January-February-March (JFM), spring as April-May-June (AMJ), and summer as July-August-September (JAS).

Figure 4 shows monthly mean sea ice motion and thickness fields from PIOMAS output, for the months of October through June averaged over the years 1979–2012. At the start of the growth season in October, sea ice in the EBS is thin and moving generally westward. The westward motion pulls ice away from Banks Island and Amundsen Gulf [*Markham*, 1975], keeping it thinner than it might otherwise be under purely thermodynamic atmospheric winter cooling. This effect continues through November and December, although with decreasing amplitude. By January, mean ice motion in the EBS has slowed considerably, a situation that persists through February and March. This quiescent period during winter allows sea ice thickness to increase via growth. By April, westward sea ice motion has returned to the EBS, a situation that continues through June [*Drobot and Maslanik*, 2003].

In the WBS, Figure 4 shows westward sea ice motion (strongest in fall and spring as for the EBS) that draws sea ice from the EBS into the region. The main difference from the EBS is that in the WBS from October through March, ice vectors also have a strong southward component. This pattern draws relatively thick ice from northeast of the Beaufort Sea (adjacent to the Canadian Arctic Archipelago) southwestward into the WBS.

Figure 5 shows monthly mean sea level pressure and 10 m surface winds from the NCEP/NCAR reanalysis, which is used to drive the PIOMAS model. In October, sea level pressure contours in the Beaufort Sea are mainly zonal, forcing easterly winds that drive the westward sea ice motion noted in Figure 4. In the following months of late fall through winter, a distinct sea level pressure maximum forms to the northwest of the Beaufort Sea, leaving relatively flat contours in the EBS region [*Markham*, 1975; *Overland*, 2009]. The result is quiescent winds in the EBS and slow ice motion (Figure 4). This situation changes rapidly in spring, when the center of the Beaufort High pressure cell broadens eastward forming a ridge that induces strong easterly winds in the EBS. In May and June, the ridge is still evident (although with a pressure maximum shifted eastward toward the Canadian Arctic Archipelago) so that easterly winds persist in the Beaufort Sea.
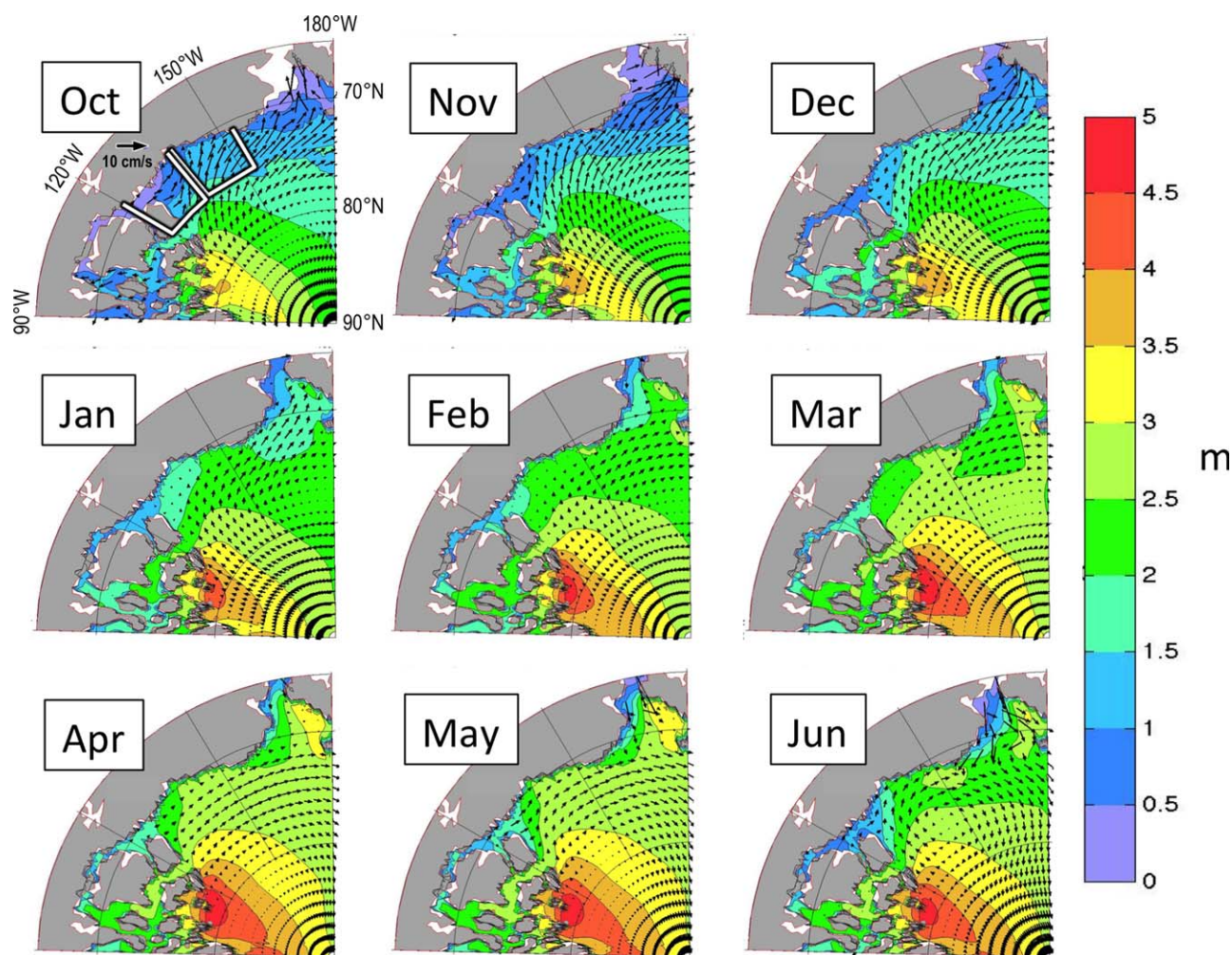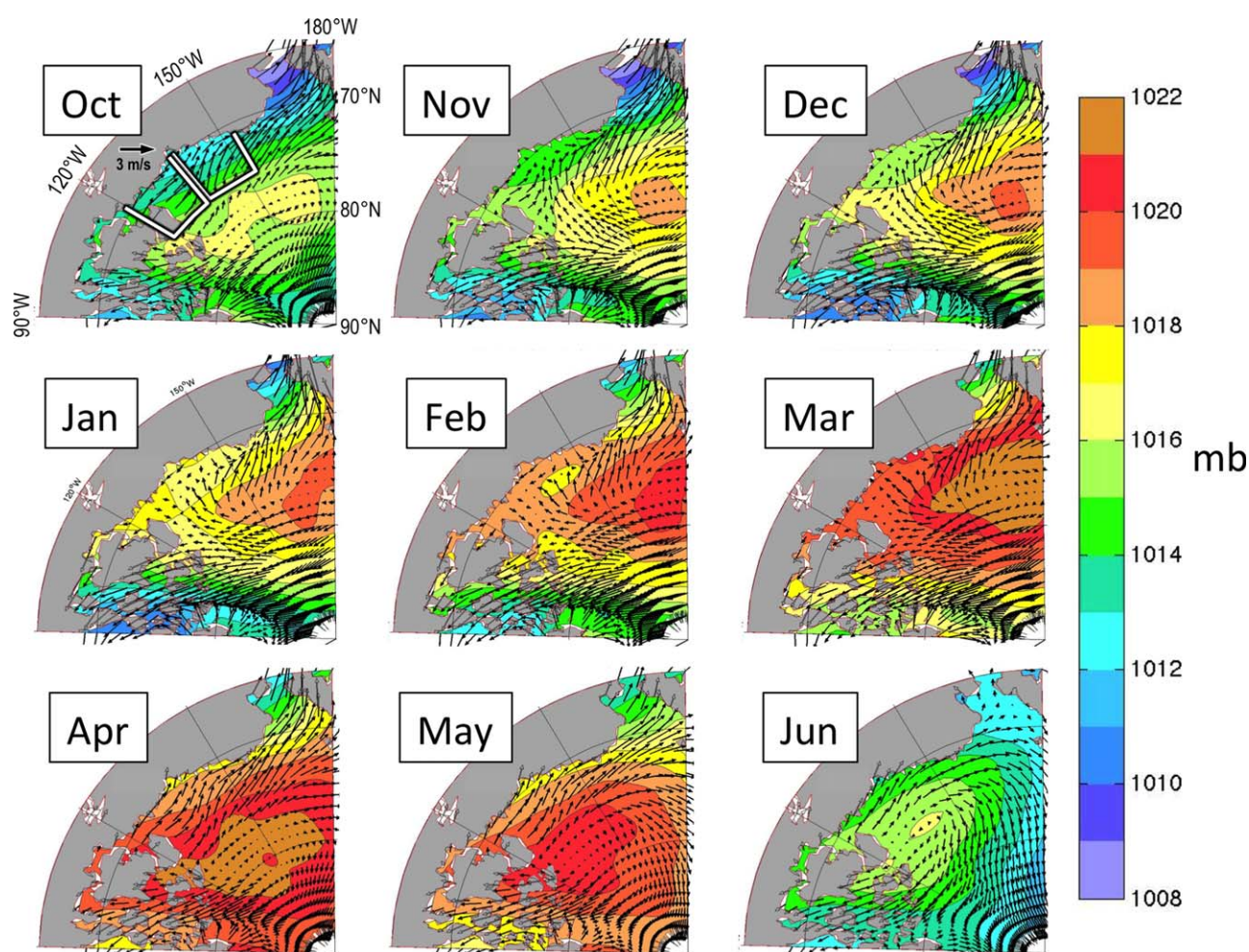
Figure 4. Monthly mean sea ice velocity (vectors) and thickness (colored contours) for October through June, from PIOMAS output averaged over 1979–2012. Also shown for October are the EBS and WBS regions (reference Figure 1).

A quantitative analysis of the modeled monthly mean thermodynamic and dynamic forcing on sea ice thickness changes in the Beaufort Sea during late winter and spring is presented in Figure 6, inspired by a similar seasonal-mean analysis presented in *Lindsay and Zhang* [2005]. In winter, ice thickness increases mainly by thermodynamic growth, although by March this growth has slowed. Dynamics also tends to increase ice thickness close to the WBS coast during the growth season [*Lindsay and Zhang*, 2005], owing to ice import from the EBS (which induces ridging against the coast via internal stress [*Steele et al.*, 1997]) and thick ice import from the Arctic Ocean areas adjacent to the Canadian Arctic Archipelago. April is still a month of net growth (although with declining amplitude), but now a strong dynamical effect is seen in the EBS. Westward ice motion forced by easterly winds (Figures 4 and 5) encourages the formation of leads (which reduces the mean ice thickness) but also induces ice deformation (which increases ice thickness). The net result in this model simulation is a mean ice thickness decline. No changes in ice concentration are yet apparent (Figure 1a), but this westward motion clearly sets up a preconditioning thinning effect on the sea ice pack.

May is a transition month, when ice is still growing (weakly) in the north but ice melting is now seen in the south. This model result is validated by satellite-based observational studies that generally find melt onset dates in the EBS during this month [*Belchansky et al.*, 2004; *Howell et al.*, 2008; *Markus et al.*, 2009]. At the same time, westward motion similar to that seen in April continues to induce ice thinning, especially in the northern EBS. By June, we see a complete transition to thermodynamic thinning (i.e., melting) over the

Figure 5. Monthly mean 10 m wind (vectors) and sea level pressure (colored contours) for October through June, from NCEP reanalysis averaged over 1979–2012 (http://www.esrl.noaa.gov/psd/data/gridded/reanalysis/). Also shown for October are the EBS and WBS regions (reference Figure 1).

entire region, with the (more or less) expected zonal symmetry and higher amplitude in the south. At this time, dynamical forcing in much of the EBS is relatively weak, although there is some ice convergence and thickening west of Banks Island.

In summary, ice opens early in the EBS (in the long-term mean) owing to wind forcing that keeps the ice there thin relative to thicker ice in the WBS. Specifically, easterly winds sweep ice away from the EBS and into the WBS during the growth season, while the mean sea ice circulation brings thick, old ice into the WBS during the same period. These advective mechanisms are generally strong in the fall, weaken in the winter, and strengthen again in the spring during the first stages of ice loss. Later stages of ice loss in spring and through summer are more strongly influenced by thermodynamic effects such as atmospheric heating (mainly, solar radiative fluxes [*Overland*, 2009]) as well as warm water discharge from the Mackenzie River [*Nghiem et al.*, 2014]).

## 4. Long-Term Trends: Moving Toward Synchrony

Figure 3c indicates that the date of EBS ice opening has no significant long-term trend, in contrast to a significant trend toward earlier DOO in the WBS. Similar results have been found in previous studies of ice concentration trends and retreat [*Barber and Hanesiak*, 2004; *Barber et al.*, 2008; *Stammerjohn et al.*, 2012; *Tivy et al.*, 2011]. In this section, we seek an explanation for this observation, focusing at first on long-term trends
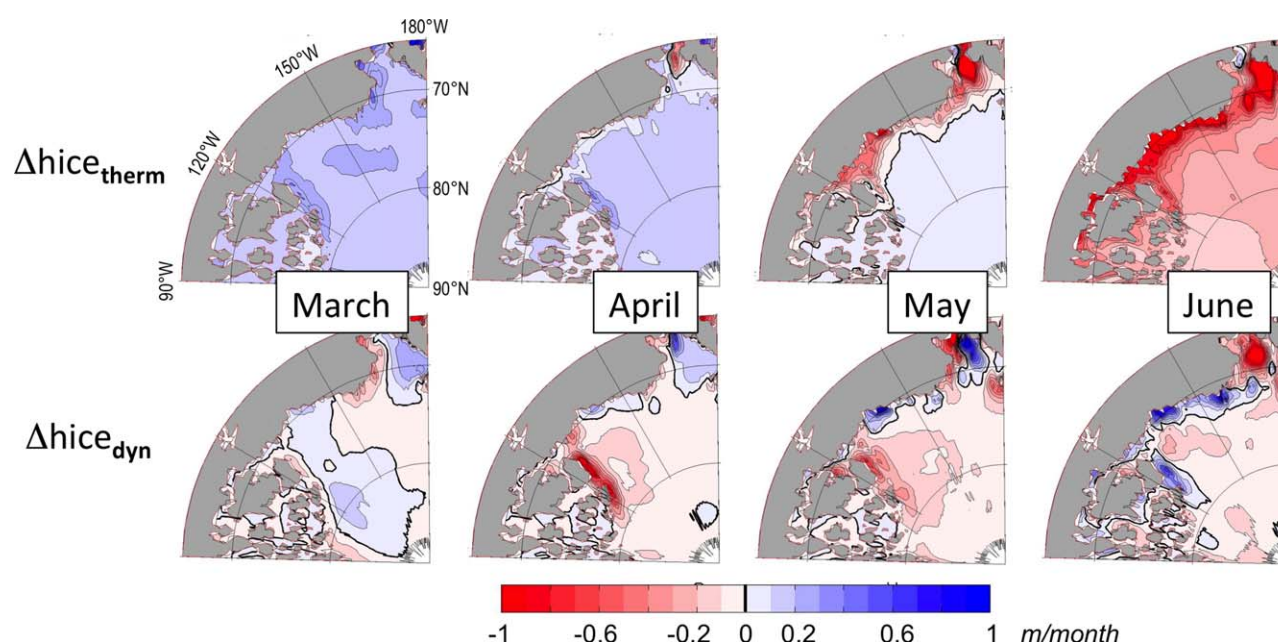
Figure 6. (top row) Monthly mean ice thickness change Δhice due to thermodynamics from PIOMAS output averaged over 1979–2012. Red indicates thickness loss (i.e., net melting) while blue indicates thickness gain (i.e., net growth). (bottom row) Similar, but for dynamical processes (i.e., advection and deformation). The largest dynamical term is generally divergence (which causes thinning marked here as red contours) or convergence (marked as blue contours).

in the factors responsible for ice opening in the EBS. We then consider larger-scale spatial patterns of DOO and DOR trends over the Beaufort and Chukchi Seas. These trends interact in interesting ways with the long-term means, leading to an increase in the synchrony of seasonal ice loss over the region.

We first consider sea ice thickness at the end of the growth season in March. This parameter integrates the thermodynamic and dynamic forcing over the growth season, and represents the initial condition for the ice loss season to come. Figure 7 shows March-average PIOMAS modeled sea ice thickness along latitude 71°N in the Beaufort Sea during 1979–2012. We see that in every year, ice is always thinner in the EBS and
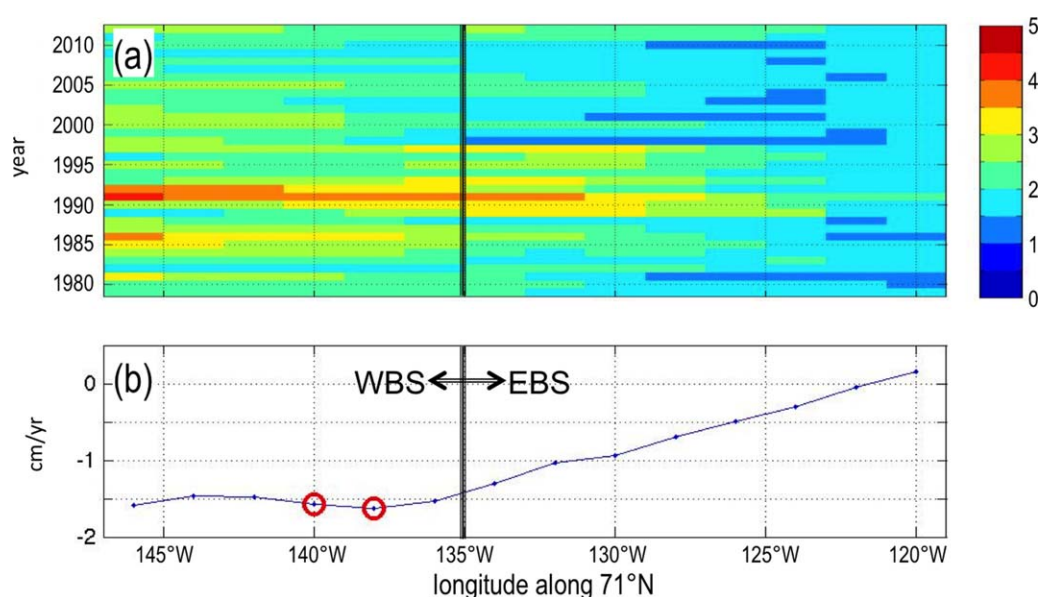
Figure 7. The variation along latitude 71°N of March mean ice thickness from PIOMAS output for (a) every year and (b) long-term linear trends over 1979–2012, with ≥95% significance marked with red circles. Longitude 135°W marks the boundary between the western Beaufort Sea (WBS) and eastern Beaufort Sea (EBS).
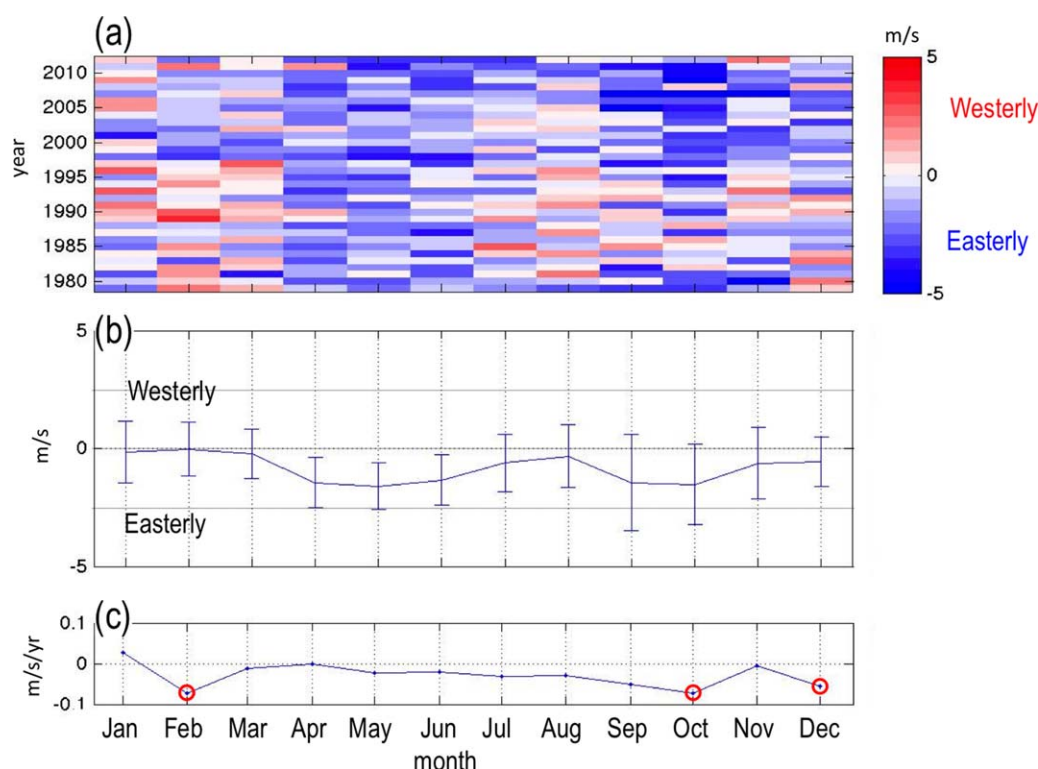
Figure 8. Monthly mean NCEP reanalysis 10 m zonal wind speed at 71°N, 130°W as in Figure 5, for (a) every year during 1979–2012, (b) long-term means (blue line) and ±1 standard deviation of interannual variability (vertical bars), and (c) long-term linear trends with ≥95% significance marked with red circles. Using the global standard, easterly winds are negative and westerly winds are positive.

thicker in the WBS, similar to the long-term mean discussed in section 3. The long-term trend is generally toward thinner ice. In the WBS, the rate is about −1.5 cm/yr and may be linked in part to a reduction in thick, multiyear ice import from the Arctic Ocean areas adjacent to the Canadian Arctic Archipelago [*Hutchings and Rigor*, 2012; *Maslanik et al.*, 2007]. The significance of the trend is negatively impacted by model uncertainty (see section 2) and in some locations by the presence of particularly thick ice in the early 1990s. Trends in the EBS (where first-year ice dominates [*Galley et al.*, 2008]) are smaller than in the WBS and insignificant, in keeping with observations in this area [*Melling et al.*, 2005]. In summary, the historically thick ice of the WBS is thinning at a more rapid rate than the historically thin ice in the EBS, which leads to a more uniform thickness throughout the Beaufort Sea.

We turn now to the thermodynamic and dynamic forcing during the spring that might influence ice-opening trends. Interannual variations in EBS net shortwave energy fluxes (not shown) are generally small [*Stroeve et al.*, 2014], with no significant spring or summer long-term trends. Figure 8 shows the zonal wind amplitude in the EBS. Easterlies are evident in the spring (with relatively small interannual variance) and in the late summer/early fall (with about twice the interannual variance as in spring). Spring and fall peaks in easterly winds are also evident in station data from the EBS coast at Tuktoyaktuk, Sachs Harbour, and Ulukhaktok (not shown). The mean amplitude of these easterly winds is comparable in spring and fall, although the resulting ice velocities are a bit weaker in spring (compare Figures 4 and 5) owing to a thicker ice cover at that time with higher internal stress that resists the wind forcing [*Steele et al.*, 1997]. Long-term trends are generally insignificant and tend in spring and summer toward stronger easterlies at a rate of less than 0.2 m/decade. Station data trends (not shown) at Tuktoyaktuk and Ulukhaktok show similar results, with generally small and insignificant trends. Spring surface winds at Sachs Harbour do show significant trends of up to 0.5 m/decade toward weakening easterlies, although by 2012 the monthly means are still easterly. Recent studies [*Spreen et al.*, 2011] have found negligible wind trends over the growth season in the Beaufort Sea.

So why is there no trend in DOO over the years 1979–2012 in the EBS? Our analysis shows that in this area, there is no particular trend in ice thickness at the end of the growth season, and there is no trend in the

easterly winds, the primary forcing for ice opening during spring. On the other hand, we do note that DOO is trending toward earlier values in the WBS (Figure 3c), which we suspect is influenced by the loss of thick multiyear ice [*Hutchings and Rigor*, 2012; *Maslanik et al.*, 2011] that (as shown in Figure 4) feeds this region during winter. The net result is that ice opening in the Beaufort Sea is trending toward a more uniform zonal pattern, i.e., the difference between early EBS opening and later WBS opening has been declining over the past 33 years and is now small (Figure 2a). Figures 9a–9d show the big picture view over our study area of the long-term mean DOO, DOR, and significant linear trends in these quantities over 1979–2012. Of course, DOR happens later than DOO, and DOO and DOR are generally later in northern areas relative to southern areas. More importantly, both DOO and DOR are earliest in the EBS and in the Chukchi Sea, while a lag of 4–6 weeks is evident in the WBS and the northern Chukchi Sea. Trends in both of these quantities show little of significance in the EBS, with stronger values in the WBS and in the northern Chukchi Sea, similar to that shown in *Stammerjohn et al.* [2012] and *Frey et al.* [2014].

The main point of interest here is that significant negative trends in DOO and DOR are strongest where their long-term means are latest. What does this mean? Focusing on the Beaufort Sea, this implies that seasonal ice concentration decline across the region is changing from a past with very different dates to a present with more synchronous ice loss. We can quantify this effect by considering the difference in DOO along 71°N averaged over longitudes 136°W–146°W (i.e., the WBS) minus the opening date for longitudes 124°W–134°W (i.e., the EBS, excluding Amundsen Gulf), using the same data as in Figure 3. The result is shown in Figure 9e. The linear least squares trend line fitted to this time series has a slope of −0.71 days/year (significantly different from zero at 95% confidence), with a value of 41 days in 1979 and only 20 days in 2012. With regard to DOR, east-west trend differences have a smaller slope of −0.24 days/yr that is not significantly different from zero, with a value in 2012 nearly identical to that for DOO, i.e., 20 days. Similar results are obtained when averaging not just along 71°N but over the EBS and WBS regions.

In summary, ice opening is becoming more synchronous across the Beaufort Sea. Ice retreat also has this tendency, although the trend is not statistically significant at this time. However, there is still a delay in the WBS relative to the EBS in both DOO and DOR, and in recent years, this delay is about the same for both parameters, i.e., ~20 days.

5. Interannual Variations: Moving Toward Predictability

Thus far, we have discussed the mean seasonal cycle of sea ice parameters in the EBS relevant to its early opening behavior (section 3) and long-term trends in DOO and DOR across the Beaufort Sea (section 4). In this section, we examine the causes of year-to-year variability in Beaufort Sea opening and retreat, and then apply our results to predicting ice loss in this area.

In the mean, ice opens early in the EBS relative to the WBS because, as discussed in section 3, spring easterly winds diverge and thus thin an ice pack that is already relatively thin at the end of the growth season. So how does interannual variability of these two factors (i.e., ice thickness at the end of the growth season and the strength of spring easterly winds) impact interannual variability of DOO and DOR? We first consider the impact of ice thickness in March. Perhaps surprisingly, we find no significant correlations in the Beaufort Sea between linearly detrended time series of PIOMAS March ice thickness and DOO or DOR. We find this result when applied separately to the EBS, the WBS, the union of the two regions, as well as for subsamples only along longitude 71°N as in previous figures. March ice thickness does vary from year to year, but its value has no statistically significant influence on DOO or DOR.

What is the explanation for this puzzle? Our interpretation is that while the thickness of sea ice at the end of winter influences seasonal ice loss in the mean, it has less bearing on interannual anomalies. These anomalies are controlled instead by anomalies in the strength of easterly winds during spring. This is illustrated in Figure 10, which shows the influence of spring winds on opening and retreat along longitude 71°N in the Beaufort Sea. Both correlations are significant. The figure shows that for any given year, an increase of 1 m/s in easterly spring winds leads to an earlier EBS DOO of ~14 days, and an earlier EBS DOR of ~18 days. Similar relationships are found in the WBS, although with ~25% smaller correlations and slopes. Similar relationships also hold when averaging over the entire EBS or WBS areas, or when using PIO-MAS modeled ice concentration to compute DOO and DOR. Finally, similar results were found when we
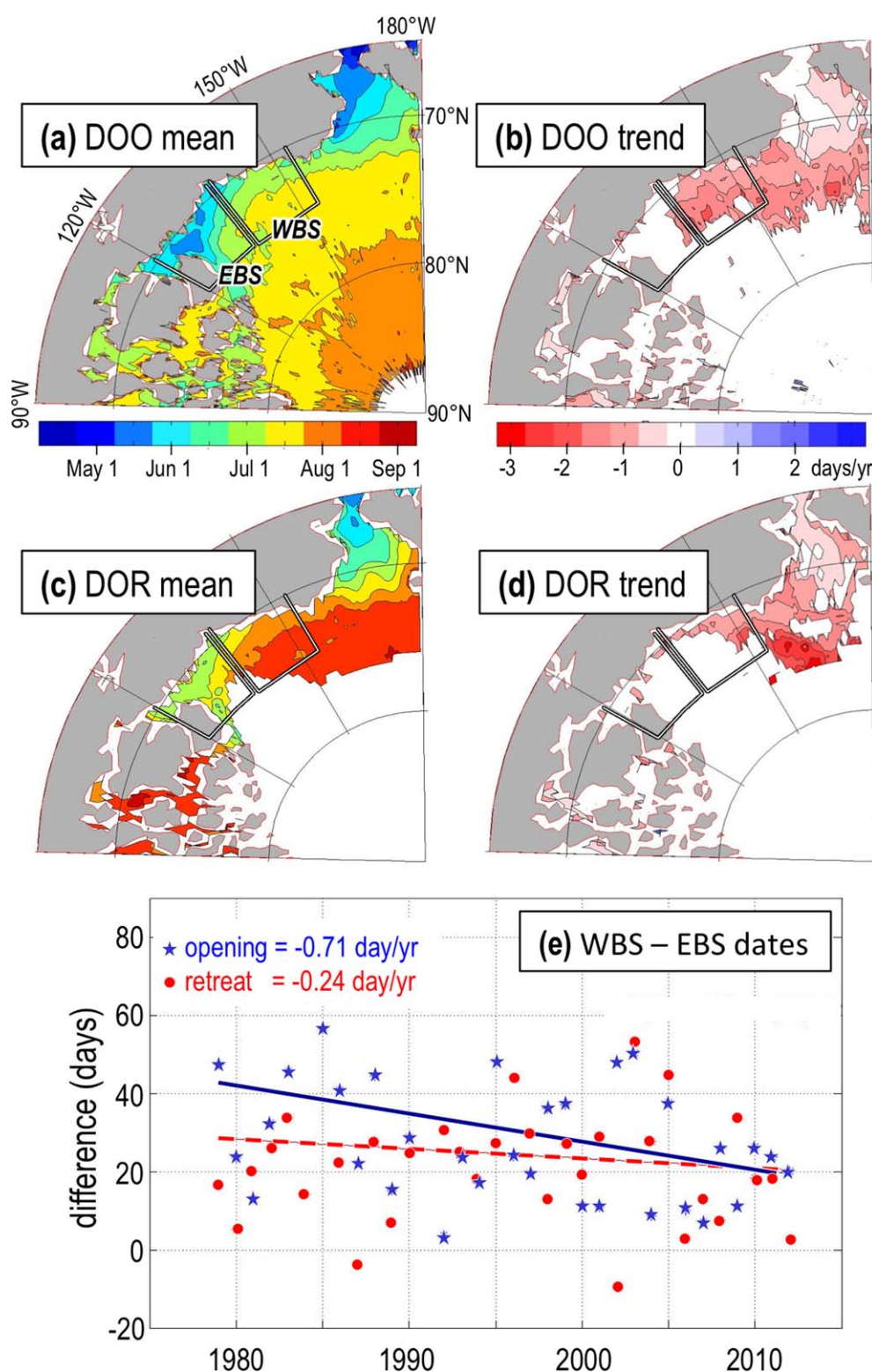
Figure 9. (a and b) Mean and ≥95% significant linear trend in the Date of Opening (DOO) over 1979–2012. (c and d) Same as Figures 9a and 9b but for Date of Retreat (DOR). (e) Long-term trends in synchrony across the Beaufort Sea, as measured by the delay (in days) in DOO or DOR in the WBS (along 71°N, 136°W–146°W), relative to DOO or DOR at the same latitude for longitudes 124°W–134°W (i.e., in the EBS excluding Amundsen Gulf). Blue stars show the difference in DOO for each year, while the blue line shows the least squares fit, whose slope is significantly different from zero with 95% confidence. Red dots and dashed red line show the same for DOR; the slope here is not significantly different from zero. Slopes in Figure 9e are similar when averaging over the entire EBS and WBS areas.
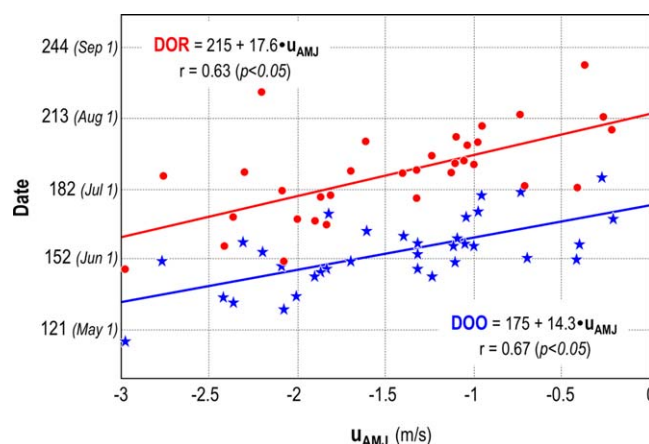
Figure 10. Day of ice Opening (DOO) and Day of ice Retreat (DOR) computed from passive microwave ice concentration data from NSIDC (as in Figure 1) versus mean spring 10 m easterly winds (u_{AMJ}) from NCEP reanalysis, for 120°W–134°W along 71°N, i.e., in the EBS. Note that, in keeping with global wind convention, easterly winds are assigned negative values. All time series linearly detrended.

extended the analysis to the year 2013 (when there were weak spring easterlies and late DOO/DOR) and the year 2014 (when there were strong spring easterlies and early DOO/DOR).

To further illustrate how spring winds influence ice loss, four case studies are shown in Figure 11. The first two columns show the evolution of monthly mean ice and wind parameters in the EBS for two growth seasons (2007/2008 and 1990/1991) with strong spring easterly winds and the associated strong westward ice motion. The difference between these two cases is that the earlier one had relatively thin end-of-winter sea ice

thickness, while the latter case exhibits quite thick ice. Yet in both of these cases, ice thickness is seen as a secondary effect relative to the strong spring easterlies, which produce rapid thinning and ice opening. (In fact, strong May 1991 winds and ice motion revert to quiescent conditions in June, resulting in a drastic slow-down in ice retreat.) Conversely, the second pair of growth seasons (1988/1989 and 2000/2001) both have relatively weak spring easterly winds and westward sea ice motion [see *Kwok*, 2006] for another view of weak westward ice motion near Amundsen Gulf), with one thick and one thin end-of-winter sea ice state. Yet in both of these cases, sea ice opening is relatively slow in response to weak spring dynamic forcing.

Figure 12 presents the linear relationship between monthly mean easterly wind magnitude and DOR. The figure also shows the 1979–2012 mean DOR and ±standard deviation of interannual variability, similar to that shown in Figure 3b for DOO. The relationship between winds and DOR is generally insignificant before spring, except for some effect in the eastern WBS from strong fall easterlies that may survive through the growth season. The largest signal is a positive relationship between monthly mean easterly winds in spring
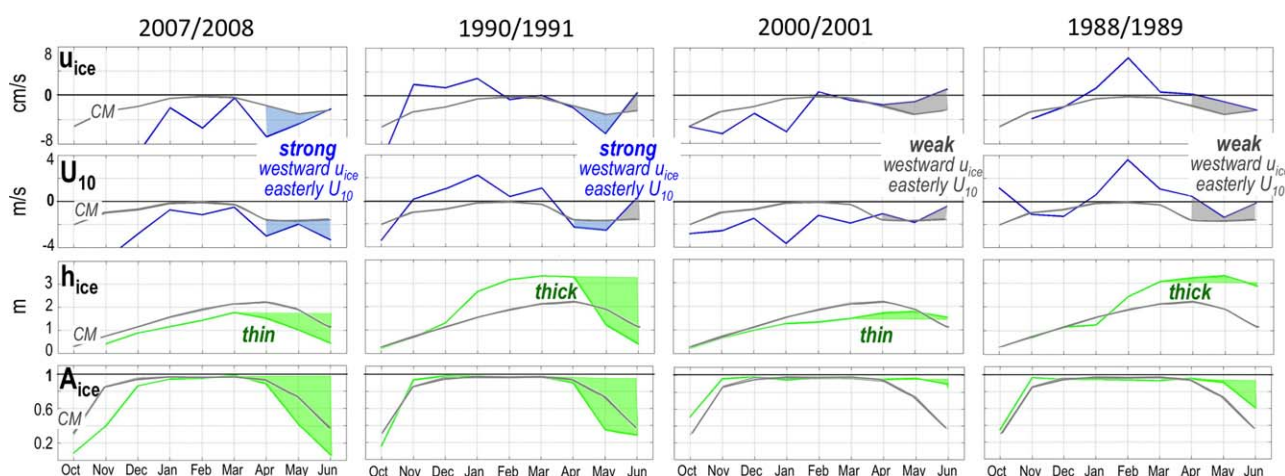
Figure 11. Four case studies at 71°N, 130°W showing the effect on ice opening of the magnitude of spring (April, May, June) easterly wind and ice motion using monthly mean data. Ice motion u_{ice} is from PIOMAS output, 10 m zonal wind speed U_{10} is from NCEP reanalysis as in Figure 5, ice thickness h_{ice} is from PIOMAS output, and ice concentration A_{ice} is from NSIDC passive microwave data as in Figure 1. The first two columns show that strong easterly winds and the resulting westward ice motion cause rapid ice opening for a year with (first column) anomalously thin or (second column) anomalously thick end-of-winter (i.e., March) ice thickness. The final two columns show that weak easterly winds and westward ice motion induce relatively weak ice opening for a year with (third column) anomalously thin or (fourth column) anomalously thick March ice thickness. The long-term climatological monthly means (CM) are given for reference in each plot (gray lines, fixed within each row). Anomalous easterly ice motion and westward winds are shaded blue, while anomalous westerly winds and eastward ice motion is shaded gray, all relative to the long-term CM. The change in ice thickness or concentration from March values is shaded green in the bottom two rows.
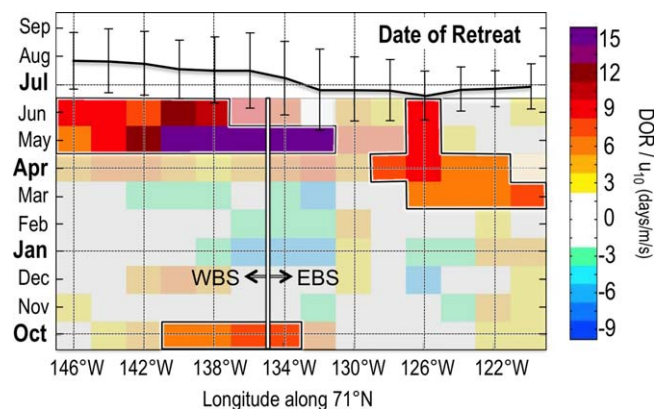
Figure 12. The slope of a regression line between DOR (computed from NSIDC passive microwave data as in Figure 1) and u$_{10}$ (the monthly mean NCEP 10 m easterly winds), for longitudes along latitude 71°N. Slopes 95% significantly different from zero are denoted with black boxes. All time series are linearly detrended. Longitude 135°W marks the boundary between the western Beaufort Sea (WBS) and eastern Beaufort Sea (EBS). At top is shown the long-term mean DOR, with vertical bars denoting ±1 standard deviation of interannual variability.

and DOR, i.e., stronger easterlies lead to earlier retreat dates. This relationship becomes significant earliest (in late winter) in the eastern part of the EBS, i.e., in Amundsen Gulf and close to Banks Island. By spring, significant slopes are seen in the rest of the EBS and in the eastern WBS.

The slopes in Figure 12 are generally smaller than in Figure 10. The reason is that strong easterlies in any month of spring are likely to induce early retreat, so correlation is enhanced by averaging over the entire season. The individual month with maximum correlation is May, when an easterly wind anomaly of 1 m/s will induce early retreat of 6–15 days.

We can also consider the lead time that anomalous easterlies provide in predicting DOR anomalies. Figure 12 indicates that the long-term mean DOR happens in early to mid-summer across the southern Beaufort Sea. This means that if we are interested in predictors that provide at least 1 month lead time, May or June easterly wind anomalies provide useful information about DOR in the WBS, which on average happens 2–3 months later in July to August. Similarly, March, April, or May easterlies provide useful information about EBS DOR, which happens on average 2–4 months later in July.

A plot like Figure 12 can be made for DOO (not shown) that has similar characteristics, except with smaller amplitudes (in keeping with Figure 10). More importantly, the mean DOO occurs in spring at the same time as the easterly wind anomalies. That is, there is very little lead time to this predictor: easterly wind anomalies produce DOO anomalies in "real time."

Thus, it seems we have a way to predict DOR anomalies (relative to the long-term mean) in the Beaufort Sea. One caveat is that we have discussed in section 4 how DOR is trending toward earlier values in the WBS. If this trend continues, then the predictive value of spring easterly wind anomalies in this area may lessen in the future.

6. Summary and Discussion

Each spring, ice opens (i.e., its concentration falls below 0.8) early in the eastern Beaufort Sea (EBS) because the ice is relatively thin there, owing to easterly offshore winds that are in the long-term mean strongest in fall and spring. There is little long-term trend in the Date of Opening (DOO) over the past 33 years in this area, owing mostly to a lack of trend in the winds. The story is very different, however, in the western Beaufort Sea (WBS), where the ice has historically been thicker and older, and opening has been later. In recent years, this ice has become younger and thinner, resulting in earlier DOO. The net effect of trends in the eastern and western Beaufort Sea is that DOO is becoming more synchronous across the entire area. The Date of Retreat (DOR, when concentration falls below 0.15) is also trending in this direction, although the trend is not statistically significant over our study period. At present, ice opening and retreat in the western Beaufort Sea still lags that in the eastern Beaufort Sea by about 20 days.

In any given year, an increase in monthly mean easterly winds during spring of ∼1 m/s induces earlier ice retreat of 6–15 days. Since DOR happens in the Beaufort Sea during summer, monthly mean spring easterly wind anomalies provide 2–4 months of lead time in predicting DOR anomalies. A similar relationship was found for DOO, but this is less useful for prediction since DOO generally occurs in spring at the same time as easterly wind anomalies. Finally, we note that as DOR trends toward earlier values in the WBS, the predictive capability discussed here may be on the decline.

STEELE ET AL.   1130

Our time series is relatively short, and strong decadal signals such as seen in Figures 3 and 7 likely influenced our calculation of linear trends. For the parameters of interest here, this effect seems stronger in the WBS relative to the EBS [*Barber et al.*, 2008]. Trends in EBS sea ice parameters are relatively small, owing mainly to a lack of wind trends in this region. However, this situation may change as the global warming signal strengthens in the coming decades.

Recent interest in arctic change has motivated an increasing number of annual research icebreaker cruises to the Beaufort Sea. In addition, there is also interest in resource development (fisheries, oil, etc.). In early summer, Figures 1 and 9 show how transit between the early opening and retreat areas of the EBS and the Chukchi Sea may be limited by lingering ice in the WBS region, similar to that encountered by explorers since the late 1800s [*Stern*, 2014]. Our study indicates that as ice opening and retreat dates become more uniform across the Beaufort Sea, this limitation might lessen in future years.

Sea ice serves as a substrate for and influence on movement, mating, hunting, and denning for some marine mammals such as seals, polar bears, and whales [*Bromaghin et al.*, 2015; *Loseto et al.*, 2006; *Regehr et al.*, 2010]. Our results indicate that the climatologically late-retreating sea ice in the WBS is trending toward earlier DOOs and DORs, which may likely affect these behaviors in this region.

Finally, we note that early opening and retreat areas have the potential to warm earlier than other, more icy regions via solar energy input [*Perovich et al.*, 2007]. This can be seen in long-term mean sea surface temperature maps of the Beaufort Sea [*Steele et al.*, 2008]. Such solar inputs affect biological productivity, and can affect the total amount of oceanic summer heating, which in turn influences fall freezeup [*Stroeve et al.*, 2014].

References

Agnew, T., and S. Howell (2003), The use of operational ice charts for evaluating passive microwave ice concentration data, *Atmos. Ocean*, *41*(4), 317–331, doi:10.3137/ao.410405.

Arrigo, K. R., and G. L. van Dijken (2004), Annual cycles of sea ice and phytoplankton in Cape Bathurst polynya, southeastern Beaufort Sea, Canadian Arctic, *Geophys. Res. Lett.*, *31*, L08304, doi:10.1029/2003GL018978.

Barber, D. G., and J. M. Hanesiak (2004), Meteorological forcing of sea ice concentrations in the southern Beaufort Sea over the period 1979 to 2000, *J. Geophys. Res.*, *109*, C06014, doi:10.1029/2003JC002027.

Barber, D. G., J. V. Lukovich, J. Keogak, S. Baryluk, L. Fortier, and G. H. R. Henry (2008), The changing climate of the Arctic, *Arctic*, *61*, 7–26.

Belchansky, G. I., D. C. Douglas, and N. G. Platonov (2004), Duration of the Arctic Sea ice melt season: Regional and interannual variability, 1979–2001, *J. Clim.*, *17*(1), 67–80.

Bromaghin, J. F., T. L. McDonald, I. Stirling, A. E. Derocher, E. S. Richardson, E. V. Regehr, D. C. Douglas, G. M. Durner, T. C. Atwood, and S. C. Amstrup (2015), Polar bear population dynamics in the southern Beaufort Sea during a period of sea ice decline, *Ecol. Appl.*, doi:10.1890/14–1129.1, in press.

Carmack, E. C., R. W. Macdonald, and S. Jasper (2004), Phytoplankton productivity on the Canadian Shelf of the Beaufort Sea, *Mar. Ecol. Prog. Ser.*, *277*, 37–50.

Cavalieri, D. J., and C. L. Parkinson (2012), Arctic sea ice variability and trends, 1979–2010, *Cryosphere*, *6*(4), 881–889, doi:10.5194/tc-6–881-2012.

Cavalieri, D. J., et al. (1992), NASA sea ice validation program for the DMSP SSM/I: Final Report, *NASA Tech. Memo. 104559*, 126 p., NASA, Washington, D. C.

Cavalieri, D. J., C. L. Parkinson, P. Gloersen, and H. Zwally (1996), Sea ice concentrations from Nimbus-7 SSMR and DMSP SSM/I-SSMIS Passive Microwave Data, Natl. Snow and Ice Data Cent., Boulder, Colo. [Updated yearly.]

Chevallier, M., D. S. Y. Melia, A. Voldoire, M. Deque, and G. Garric (2013), Seasonal forecasts of the Pan-Arctic sea ice extent using a GCM-based seasonal prediction system, *J. Clim.*, *26*(16), 6092–6104, doi:10.1175/JCLI-D-12–00612.1.

Comiso, J. C., and D. K. Hall (2014), Climate trends in the Arctic as observed from space, *Wires Clim. Change*, *5*(3), 389–409.

Drobot, S. D., and J. A. Maslanik (2003), Interannual variability in summer Beaufort Sea ice conditions: Relationship to winter and summer surface and atmospheric variability, *J. Geophys. Res.*, *108*(C7), 3233, doi:10.1029/2002JC001537.

Frey, K. E., J. A. Maslanik, J. Clement-Kinney, and W. Maslowski (2014), Recent variability in sea ice cover, age, and thickness in the Pacific Arctic Region, in *The Pacific Arctic Region: Ecosystem Status and Trends in a Rapidly Changing Environment*, edited by J. M. G. A. W. Maslowski, Springer, Dordrecht, Netherlands, doi:10.1007/978-94-017–8863-2_3.

Galley, R. J., E Key, D. G. Barber, B. J. Hwang, and J. K. Ehn (2008), Spatial and temporal variability of sea ice in the southern Beaufort Sea and Amundsen Gulf: 1980–2004, *J. Geophys. Res.*, *113*, C05S95, doi:10.1029/2007JC004553.

Galley, R. J., B. G. T. Else, S. E. L. Howell, J. V. Lukovich, and D. G. Barber (2012), Landfast sea ice conditions in the Canadian Arctic: 1983–2009, *Arctic*, *65*(2), 133–144.

Howell, S. E. L., A. Tivy, J. J. Yackel, B. G. T. Else, and C. R. Duguay (2008), Changing sea ice melt parameters in the Canadian Arctic Archipelago: Implications for the future presence of multiyear ice, *J. Geophys. Res.*, *113*, C09030, doi:10.1029/2008JC004730.

Hutchings, J. K., and I. G. Rigor (2012), Role of ice dynamics in anomalous ice conditions in the Beaufort Sea during 2006 and 2007, *J. Geophys. Res.*, *117*, C00E04, doi:10.1029/2011JC007182.

Kalnay, E., et al. (1996), The NCEP/NCAR 40-year reanalysis project, *Bull. Am. Meteorol. Soc.*, *77*(3), 437–471.

Kwok, R. (2006), Exchange of sea ice between the Arctic Ocean and the Canadian Arctic Archipelago, *Geophys. Res. Lett.*, *33*, L16501, doi:10.1029/2006GL027094.

Laxon, S. W., et al. (2013), CryoSat-2 estimates of Arctic sea ice thickness and volume, *Geophys. Res. Lett.*, *40*(4), 732–737, doi:10.1002/grl.50193.

Lindsay, R. W. (1998), Temporal variability of the energy balance of thick Arctic pack ice, *J. Clim.*, *11*(3), 313–333.

Lindsay, R. W., and J. Zhang (2005), The thinning of Arctic sea ice, 1988–2003: Have we passed a tipping point?, *J. Clim.*, *18*(22), 4879–4894.

Loseto, L. L., P. Richard, G. A. Stern, J. Orr, and S. H. Ferguson (2006), Segregation of Beaufort Sea beluga whales during the open-water sea-son, *Can. J. Zool.*, *84*(12), 1743–1751, doi:10.1139/z06–160.

Lukovich, J. V., and D. G. Barber (2005), On sea ice concentration anomaly coherence in the southern Beaufort Sea, *Geophys. Res. Lett.*, *32*, L10705, doi:10.1029/2005GL022737.

Markham, W. E. (1975), Ice climatology of the Beaufort Sea, *Beaufort Sea Tech. Rep. 26*, 87 pp., Dept. of the Environ., Victoria, B. C., Canada.

Markus, T., J. C. Stroeve, and J. Miller (2009), Recent changes in Arctic sea ice melt onset, freezeup, and melt season length, *J. Geophys. Res.*, *114*, C12024, doi:10.1029/2009JC005436.

Maslanik, J., C. Fowler, J. Stroeve, S. Drobot, J. Zwally, D. Yi, and W. Emery (2007), A younger, thinner Arctic ice cover: Increased potential for rapid, extensive sea-ice loss, *Geophys. Res. Lett.*, *34*, L24501, doi:10.1029/2007GL032043.

Maslanik, J., J. Stroeve, C. Fowler, and W. Emery (2011), Distribution and trends in Arctic sea ice age through spring 2011, *Geophys. Res. Lett.*, *38*, L13502, doi:10.1029/2011GL047735.

Melling, H., D. A. Riedel, and Z. Gedalof (2005), Trends in the draft and extent of seasonal pack ice, Canadian Beaufort Sea, *Geophys. Res. Lett.*, *32*, L24501, doi:10.1029/2005GL024483.

Nghiem, S. V., D. K. Hall, I. Rigor, P. Li, and G. Neumann (2014), Effects of Mackenzie River discharge and bathymetry on sea ice in the Beau-fort Sea, *Geophys. Res. Lett.*, *41*, 873–879, doi:10.1002/2013GL058956.

Overland, J. E. (2009), Meteorology of the Beaufort Sea, *J. Geophys. Res.*, *114*, C00A07, doi:10.1029/2008JC004861.

Overland, J. E., and M. Y. Wang (2013), When will the summer Arctic be nearly sea ice free?, *Geophys. Res. Lett.*, *40*, 2097–2101, doi:10.1002/grl.50316.

Perovich, D. K., B. Light, H. Eicken, K. F. Jones, K. Runciman, and S. V. Nghiem (2007), Increasing solar heating of the Arctic Ocean and adja-cent seas, 1979–2005: Attribution and role in the ice-albedo feedback, *Geophys. Res. Lett.*, *34*, L19505, doi:10.1029/2007GL031480.

Peterson, I. K., S. J. Prinsenberg, and J. S. Holladay (2008), Observations of sea ice thickness, surface roughness and ice motion in Amundsen Gulf, *J. Geophys. Res.*, *113*, C06016, doi:10.1029/2007JC004456.

Regehr, E. V., C. M. Hunter, H. Caswell, S. C. Amstrup, and I. Stirling (2010), Survival and breeding of polar bears in the southern Beaufort Sea in relation to sea ice, *J. Animal Ecol.*, *79*(1), 117–127, doi:10.1111/j.1365–2656.2009.01603.x.

Schweiger, A., R. Lindsay, J. L. Zhang, M. Steele, H. Stern, and R. Kwok (2011), Uncertainty in modeled Arctic sea ice volume, *J. Geophys. Res.*, *116*, C00D06, doi:10.1029/2011JC007084.

Simpson, K. G., J. E. Tremblay, and N. M. Price (2013), Nutrient dynamics in the Western Canadian Arctic. I. New production in spring inferred from nutrient draw-down in the Cape Bathurst Polynya, *Mar. Ecol. Prog. Ser.*, *484*, 33–45, doi:10.3354/meps10275.

Snape, T. J., and P. M. Forster (2014), Decline of Arctic sea ice: Evaluation and weighting of CMIP5 projections, *J. Geophys. Res. Atmos.*, *119*, 546–554, doi:10.1002/2013JD020593.

Spreen, G., R. Kwok, and D. Menemenlis (2011), Trends in Arctic sea ice drift and role of wind forcing: 1992–2009, *Geophys. Res. Lett.*, *38*, L19501, doi:10.1029/2011GL048970.

Stammerjohn, S., R. Massom, D. Rind, and D. Martinson (2012), Regions of rapid sea ice change: An inter-hemispheric seasonal comparison, *Geophys. Res. Lett.*, *39*, L06501¸ doi:10.1029/2012GL050874.

Steele, M., J. L. Zhang, D. Rothrock, and H. Stern (1997), The force balance of sea ice in a numerical model of the Arctic Ocean, *J. Geophys. Res.*, *102*(C9), 21,061–21,079.

Steele, M., W. Ermold, and J. L. Zhang (2008), Arctic Ocean surface warming trends over the past 100 years, *Geophys. Res. Lett.*, *35*, L02614, doi:10.1029/2007GL031651.

Stern, H. (2014), Sea ice in the western portal of the Northwest Passage from 1778 to the 21st century, in *Arctic Ambition: Captain Cook and the Northwest Passage*, edited by James K. Barnett and David L. Nicandri, pp. 330–356, Univ. of Wash. Press, Seattle, Wash.

Stroeve, J., T. Markus, L. Boisvert, J. Miller, and A. Barrett (2014), Changes in Arctic melt season and implications for sea ice loss, *Geophys. Res. Lett.*, *41*, 1216–1225, doi:10.1002/2013GL058951.

Tivy, A., S. E. L. Howell, B. Alt, S. McCourt, R. Chagnon, G. Crocker, T. Carrieres, and J. J. Yackel (2011), Trends and variability in summer sea ice cover in the Canadian Arctic based on the Canadian Ice Service Digital Archive, 1960–2008 and 1968–2008, *J. Geophys. Res.*, *116*, C06027, doi:10.1029/2011JC007248.

Williams, W. J., and E. C. Carmack (2008), Combined effect of wind-forcing and isobath divergence on upwelling at Cape Bathurst, Beaufort Sea, *J. Mar. Res.*, *66*(5), 645–663.

Zhang, J. L., and D. A. Rothrock (2003), Modeling global sea ice with a thickness and enthalpy distribution model in generalized curvilinear coordinates, *Mon. Weather Rev.*, *131*(5), 845–861.

Zhang, J. L., R. Lindsay, A. Schweiger, and I. Rigor (2012), Recent changes in the dynamic properties of declining Arctic sea ice: A model study, *Geophys. Res. Lett.*, *39*, L20503, doi:10.1029/2012GL053545.